Targeted nanomedicine for prostate cancer therapy: docetaxel and curcumin co-encapsulated lipid–polymer hybrid nanoparticles for the enhanced anti-tumor activity *in vitro* and *in vivo*

Jieke Yan, Yuzhen Wang, Xufeng Zhang, Shuangde Liu, Chuan Tian & Hongwei Wang

RESEARCH ARTICLE

Targeted nanomedicine for prostate cancer therapy: docetaxel and curcumin co-encapsulated lipid–polymer hybrid nanoparticles for the enhanced anti-tumor activity *in vitro* and *in vivo*

Jieke Yan[1], Yuzhen Wang[2], Xufeng Zhang[1], Shuangde Liu[1], Chuan Tian[1], and Hongwei Wang[1]

[1]Department of Renal Transplantation, The Second Hospital of Shandong University, Ji'nan, Shandong, PR China and [2]Clinical Department, Jinan Vocation College of Nursing, Ji'nan, Shandong, PR China

Abstract

Objective: Docetaxel (DTX) remains the only effective drug for prolonging survival and improving quality of life of metastatic castration-resistant prostate cancer (mCRPC) patients. Combination anticancer therapy encapsulating DTX and another extract of traditional Chinese medicine is one nano-sized drug delivery system promising to generate synergistic anticancer effects, to maximize the treatment effect, and to overcome multi-drug resistance. The purpose of this study is to construct lipid–polymer hybrid nanoparticles (LPNs) as nanomedicine for co-encapsulation of DTX and curcumin (CUR).
Methods: DTX and CUR co-encapsulated LPNs (DTX-CUR-LPNs) were constructed. DTX-CUR-LPNs were evaluated in terms of particles size, zeta potential, drug encapsulation, and drug delivery. The cytotoxicity of the LPNs was evaluated on PC-3 human prostate carcinoma cells (PC3 cells) by MTT assays. *In vivo* anti-tumor effects were observed on the PC3 tumor xenografts in mice.
Results: The particle size of DTX-CUR-LPNs was 169.6 nm with a positive zeta potential of 35.7 mV. DTX-CUR-LPNs showed highest cytotoxicity and synergistic effect of two drugs in tumor cells in vitro. In mice-bearing PC-3 tumor xenografts, the DTX-CUR-LPNs inhibited tumor growth to a greater extent than other contrast groups, without inducing any obvious side effects.
Conclusion: According to these results, the novel nanomedicine offers great promise for the dual drugs delivery to the prostate cancer cells, showing the potential of synergistic combination therapy for prostate cancer.

Introduction

Prostate cancer (PCa) is the most frequently diagnosed cancer and the sixth leading cause of cancer-related death in males; and PCa rates are 2–5 times higher in developed countries compared with developing countries (Jemal et al., 2011; Li et al., 2012). Based on the NCCN guidelines for PCa, docetaxel (DTX) is the standard chemotherapy and the only treatment demonstrated to increase overall survival for advanced PCa (Berthold et al., 2008; Hoang et al., 2014).

DTX is a microtubule inhibitor leading to mitotic arrest in the G2/M phase of the cell cycle and ultimately to cell death. DTX was approved by the US FDA as the mainstay treatment against hormone refractory prostate cancer (van Oosterom et al., 1995; Galsky et al., 2010). Taxotere® (Sanofi-Aventis, Bridgewater, NJ) is the only commercial formulation of DTX on the market, which contains polysorbate 80 and dehydrated alcohol. However, its clinical application is limited by its multidrug resistance (MDR), highly lipophilic and practically insoluble in water, and severe toxic side effects from DTX and its excipients (Bissett et al., 1993; Vaishampayan et al., 2008; Luo et al., 2010; Zhu et al., 2015; Zu et al., 2015). Therefore, strategies (such as novel combination therapies or nanocarriers delivery systems) to increase its anti-tumor efficacy and decrease its side effects are critically needed.

Combination therapy is increasingly used as a primary cancer treatment regimen to avoid the poor response and resistance often associated with monotherapy (Mehta et al., 2012; Yang et al., 2015). Several reports have established that endoplasmic reticulum (ER) stress can facilitate persistent tumor growth and their therapeutic resistance (Healy et al., 2009; Wu et al., 2009; Schonthal, 2012; Mathur et al., 2014). Curcumin (CUR), the active component of *Curcuma longa*, has been shown inhibit the PI3K/AKT pathway and induce low levels of ER-stress specifically in cancer cells (Woo et al., 2003; Lin et al., 2008). Moreover, various researches have

Address for correspondence: Hongwei Wang, Department of Renal Transplantation, The Second Hospital of Shandong University, No. 247 Beiyuan Street, Ji'nan 250355, Shandong Province, People's Republic of China. Email: wanghongweisdu@hotmail.com

proven CUR's efficacy for PCa and nanotechnology has been applied (Horie, 2012; Sundram et al., 2012; Wei et al., 2013; Dorai et al., 2014; Eom et al., 2014; Yallapu et al., 2014; Chen et al., 2015; Guo et al., 2015). The therapeutic prospect of curcumin (CUR) in treating prostate cancer, especially for castration-resistant prostate cancer, has been evidenced in several cell culture systems and human xenograft mouse models (Chen, 2015). On one hand, the molecular mechanism of CUR induced cytotoxicity in prostate cancer cells possess multiple targets including inhibition of cyclin D1 and upregulation of p53, leading to cell cycle arrest at G1/S phase; downregulation of NF-κB and P-glycoprotein; and inhibition of androgen receptor activated epidermal growth factor receptor (EGFR) and human epidermal growth factor receptor 2 expression involved in HRPC proliferation, etc. On the other hand, aberrant activation of multiple cellular signaling pathways such as p53, NF-κB, PI3K-Akt, and IL-6/STAT3 is associated with docetaxel resistance as well (Liu et al., 2013; Zhu et al., 2015). Therefore, CUR could decrease hormone refractory (HR) PC aggressive proliferation and potentiate activity of DTX therapy, and prevent PC cell resistance to DTX. Despite CUR's significant therapeutic value, its drawbacks hindered the clinical use: extreme degradation and metabolization, insoluble in water and low bioavailability (Burgos-Morón et al., 2010). Therefore, lipid–polymer hybrid nanoparticles (LPNs) were designed to co-delivery DTX and CUR.

LPNs, which combine the characteristics of both polymeric nanoparticles and liposomes, are composed of three components: (1) a polymer core in which the therapeutic agents are encapsulated; (2) an inner lipid layer enveloping the polymer core, the main function of which is to confer biocompatibility to the polymer core; and (3) an outer lipid-PEG layer as a stealth coating that prolongs *in vivo* circulation time. Based on their unique structure, LPNs exhibit high structural integrity, stability during storage, controlled release, and high biocompatibility and bioavailability (Hadinoto et al., 2013).

In this present research, DTX and CUR co-encapsulated LPNs (DTX-CUR-LPNs) were structured. Particles size, zeta potential, drug encapsulation, and drug delivery were evaluated. Cytotoxicities of the LPNs were evaluated on PC-3 human prostate carcinoma cells (PC3 cells) by MTT assays. *In vivo* anti-tumor effects were observed on the PC3 tumor xenografts in mice. We expected LPNs co-delivery DTX and CUR were the ideal platform to enhance therapeutic efficacy and decrease toxicity.

Materials and methods

Materials

DTX and CUR was purchased from Shaanxi Pioneer Biotech Co., Ltd (Xi'an, China). Cholesterol and (3-[4,5-dimehyl-2-thiazolyl]-2,5-diphenyl-2H-tetrazolium bromide (MTT) were purchased from Sigma-Aldrich Co., Ltd (St Louis, MO). PEG-DSPE was provided by Xi'an Ruixi Biological Technology Co., Ltd (Xi'an, China). Poly (lactic-*co*-glycolic acid) (PLGA, molar ratio of D,L-lactic to glycolic acid, 50:50) was purchased from Ji'nan Daigang Biotechnology Co. Ltd (Ji'nan, China).

Cells and animals

Human PC3 prostate adenocarcinoma cells (American Type Culture Collection, Manassas, VA) were cultured in Dulbecco's Modified Eagle Medium (DMEM) with 10% fetal bovine serum (FBS) at 37 °C and 5% CO_2.

Balb/c nude mice (Shanghai Slack Laboratory Animal Co., Ltd., Shanghai, China) were purchased at 8 weeks of age and housed in ventilated cages at temperatures between 19 and 22 °C and a relative humidity of 50–60% (Eggen et al., 2014). The animal experiments were performed according to the requirements of the National Act on the Use of Experimental Animals (P. R. China) and the protocols were approved by the Animal Ethics Committee of Shandong University.

Preparation and characterization of DTX-CUR-LPNs

DTX-CUR-LPNs were prepared using a nanoprecipitation technique combined with self-assembly (Zhang et al., 2008; Chan et al., 2009). DTX (50 mg), CUR (100 mg), and PLGA (200 mg) were first dissolved in acetonitrile (10 mL). Lecithin and PEG-DSPE (2:1, molar ratio) were dissolved in a 4% ethanol aqueous solution at 20% of the PLGA polymer weight and heated to 60 °C. The drugs and PLGA acetonitrile solution were then added into the preheated lipid aqueous solution drop-wise (1 mL/min) under gentle stirring followed by vortexing for 3 min. The nanoparticles were allowed to self-assemble for 2 h with continuous stirring while the organic solvent was allowed to evaporate. The remaining organic solvent and free molecules were removed by washing the nanoparticle solution three times and then resuspended in water to obtain the final desired DTX-CUR-LPNs. The DTX-CUR-LPNs were used immediately, or stored at 2–8 °C for later use. DTX-encapsulated LPNs (DTX-LPNs), CUR-encapsulated LPNs (CUR-LPNs), and LPNs without drug (LPNs) were prepared using the same method. The DTX and CUR co-encapsulated PLGA nanoparticles (DTX-CUR-NPs) without the lipid shell were prepared by the same procedure without adding lecithin and PEG-DSPE. The amount and weight ratio of DTX and CUR added in the LPNs system was designed and optimized in the in terms of size and cytotoxicity efficiency.

The mean diameter, polydispersity index (PDI), and zeta potential of different NLCs formulations were measured using a Zetasizer Nano-ZS (Malvern Instruments, Worceshtire, UK) (Liu et al., 2015).

Drug encapsulation, drug-loading capacity, and release study of DTX-CUR-LPNs

The DTX and CUR encapsulation efficiency (EE) and loading capacity (DL) were determined as follows (Jin et al., 2014): 500 μL of drug-loaded LPNs and 1 mL of THF were transferred to a 25 mL volumetric flask, sonicated at 180 W for 10 min in an ultrasonic bath, and then diluted with mobile phase. The DTX and CUR concentration in the resulting solution was then determined by HPLC. For DTX, Chromatographic analysis was performed using a Hitachi L-2130 pump and a Hitachi L-2400 UV–Vis detector (Hitachi Inc., Tokyo, Japan) operated at a wavelength of 230 nm, using a Unitary C18 column. A mobile phase of acetonitrile and

water (60/40, v/v) was selected. The flow rate was set at 1 mL/min. For CUR, the amount of free and entrapped CUR was determined by dissolving the supernatant with a known amount of ethanol (1:10, v/v) (Saengkrit et al., 2014). The isocratic condition using mobile phase composed of 43% (w/w) acetonitrile and 57% of 1% (w/w) acetic acid in water. The flow rate was 1.0 mL/min, the injection volume was 20 μL, and monitored at 428 nm. The EE (%) and DL (%) were calculated by applying equation as follows (Hajikarimi et al., 2014): EE (%) = weight of drug in nanocarriers/ weight of feeding drug × 100; DL (%) = (weight of total drug − weight of free drug)/(weight of total drug loaded nanocarriers) × 100.

The *in vitro* drug release of DTX-CUR-LPNs, DTX-CUR-NPs, DTX-LPNs, and CUR-LPNs were performed by dialysis diffusion (Jin et al., 2014). The different LPNs were placed in the dialysis bags (MWCO: 14 000). These bags were immersed in tubes filling with 15 mL PBS (pH 7.4, containing 0.5% w/v Tween 80). Subsequently, the tubes were placed in a shaking incubator at a shaking speed of 100 rpm under 37 °C. All release media were replaced with fresh PBS at predetermined intervals to measure the drug concentration. The concentrations of DTX and CUR were measured by HPLC mentioned in the previous paragraph.

Cytotoxicity studies of DTX-CUR-LPNs

The *in vitro* cellular toxicity of DTX-CUR-LPNs, DTX-CUR-NPs, DTX-LPNs, and CUR-LPNs was studied on PC3 cells using the MTT toxicity assay, and the results are depicted in Figure 3 (Chandratre & Dash, 2015). The cells were split and plated in 96-well plates having the seeding densities of 3000 cells/well and were incubated in a humidified chamber at 37 °C in an atmosphere of 5% CO_2. After 24 h of plating, different concentrations of treatment solutions consisting of different LPNs, and free drug solution were prepared. All the plates were incubated in the presence of transient exposure for 4 h. After the incubation period, the treatment along with the media was removed from each well and was replaced with fresh media. The plates were incubated over a period of 72 h. Then the cells were treated with 30 μL of MTT solution (5 mg/mL) prepared in PBS and incubated for additional 4 h. The MTT treatment was then removed and the cells were washed and treated with a solution of 20% (w/v) SDS solution: dimethylformamide in the ratio of 1:1. All the plates were kept on the incubator shaker (MaxQ 4450, Thermo Scientific, Waltham, MA) for 45 min at 37 °C and were then analyzed on the microplate reader (Model 680, BIO-RAD, Hercules, CA) at 540 nm. The drug concentration causing 50% of cells inhibition (IC_{50}) was calculated.

In vivo anti-tumor studies of DTX-CUR-LPNs

To establish human prostate cancer xenografts, PC3 cells (4×10^6 cells/100 μL) were subcutaneously injected into the right flank of the Balb/c nude mice (Yang et al., 2015). When PC3 xenograft tumor volumes were about 100 mm^3, mice were randomly divided into eight groups (eight mice per group) to receive one of the following treatments: DTX-CUR-LPNs, DTX-CUR-NPs, DTX-LPNs, CUR-LPNs, free DTX, free CUR, LPNs, and 0.9% Saline. These treatments were performed on days 0, 7, and 14 by tail injection, the DTX dose was 5 mg/kg and the CUR was 10 mg/kg. Tumor volumes were measured and calculated every 3 d until day 21 using the formula $V = (L \times W^2)/2$, where W and L refer to the shortest and longest diameters, respectively.

The antitumor efficacy of each formulation was evaluated by tumor inhibition rate (TIR), which was calculated using the formula TIR (%) = (tumor weight of sample group − tumor weight of control group)/tumor weight of control group × 100

Statistical analysis

Measurements were carried out in triplicate. Quantitative data were presented as means ± standard deviation (SD). The analysis of variance is completed using a one-way ANOVA. $p < 0.05$ was considered statistically significant.

Results and discussion

Characterization of DTX-CUR-LPNs

Nanotechnology is a promising tool to significantly enhance antitumor efficiency of drugs (Hoang et al., 2014). The integration of chemotherapeutics with nanotechnology using drug delivery systems promises selective delivery of chemotherapeutic agents. These nano-sized drug delivery nanomedicines have advantages in comparison with systemic chemotherapy. Nanoparticles are known to exploit the enhanced permeability and retention (EPR) effect for targeting to tumors thereby increasing tumor drug concentrations while minimizing systemic toxicity.

The mean diameter and zeta potential of various kinds of LPNs are depicted in Table 1. The mean particle size ranged from 160 to 170 nm for drug-free LPNs to dual-drug-loaded LPNs. The DTX-CUR-NPs had a size of 116 nm. These data illustrated with the single drug or dual drugs loading, the particle sizes remained in the same range. However, for the nanocarriers without the lipid shell, the size is significantly smaller ($p < 0.05$). The zeta potential of DTX-CUR-LPNs was significant lower than drug-free LPNs, decreased form −19 mV to −36 mV. These may be explained by the negatively charged drugs that reduce the charge of the particles.

Table 1. Characterization of various kinds of LPNs.

LPNs	Mean diameter (nm)	PDI	Zeta potential (mV)	DTX EE (%)	CUR EE (%)	DTX DL (%)	CUR DL (%)
DTX-CUR-LPNs	169.6 ± 4.6	0.16 ± 0.06	−35.7 ± 1.9	89.8 ± 3.1	81.9 ± 5.6	5.5 ± 0.8	5.8 ± 0.6
DTX-CUR-NPs	116.4 ± 2.2	0.08 ± 0.02	−31.1 ± 2.9	80.2 ± 4.3	72.5 ± 3.6	8.3 ± 1.2	9.6 ± 1.7
DTX-LPNs	167.2 ± 3.9	0.13 ± 0.04	−26.4 ± 2.7	88.3 ± 2.9	NA	9.1 ± 1.4	NA
CUR-LPNs	168.1 ± 4.2	0.14 ± 0.05	−23.2 ± 2.3	NA	82.6 ± 3.9	NA	10.4 ± 1.9
LPNs	163.3 ± 3.8	0.11 ± 0.03	−18.5 ± 1.6	NA	NA	NA	NA

Drug encapsulation, drug loading, and release study

The lipid shell presented at the surface of the drug-loaded PLGA core may serve two distinct functions: (1) to prevent small drug molecules from freely diffusing out of the PLGA core, thereby improving drug encapsulation yield and loading yield; (2) to reduce the water penetration rate into the PLGA core, thereby decreasing the rate of hydrolysis of PLGA polymers resulting in slower drug release from the nanocarriers (Zhang et al., 2008). To test these hypotheses, DTX-CUR-NPs without the lipid shell were applied as contrast for the DTX-CUR-LPNs.

The DTX and CUR EE of DTX-CUR-LPNs were about 89% and 82%, respectively (Table 1). The DTX and CUR EE of DTX-CUR-NPs were about 80% and 73%, respectively, significantly lower than their LPN counterparts. This could be the evidence of the prevention effect of LPNs' lipid core, less small drug molecules could freely diffuse out of the PLGA core, thereby improving drug encapsulation yield. There was no obvious difference in EE between DTX-CUR-LPNs and single drug-encapsulated LPNs (DTX-LPNs and CUR-LPNs), indicating the outstanding drug encapsulation ability of LPNs to load two different drugs.

Several factors such as physicochemical properties of entrapped drugs, nature of the core, strength of the interactions between the drugs, and the core materials play an important role in governing the drug release pattern from a delivery system (Chandratre & Dash, 2015). The *in vitro* release of DTX and CUR from different LPNs systems are shown in Figures 1 and 2, separately. Figure 1 shows that the release of DTX from DTX-CUR-LPNs was significantly slower ($p < 0.05$) than the release from DTX-CUR-NPs. The same situations are found in Figure 2. The release profiles indicated that the LPNs have the more sustained behavior than PLGA NPs, this may be due to the lipid surface that hindered the release of the drugs from the PLGA core. However, the drug release from the single drug-encapsulated LPNs are similar with the dual-drug co-encapsulated DTX-CUR-LPNs.

In vitro cytotoxicity assays of LPNs

To investigate whether the enhanced cell uptake could achieve by DTX-CUR-LPNs and increased anticancer activity, the *in vitro* antitumor efficacy of free drugs, single-drug encapsulated LPNs, non-lipid shelled DTX-CUR-NPs, and DTX-CUR-LPNs were compared in PC3 prostate cancer cells by MTT assay (Yang et al., 2015). The free drugs, drug-encapsulated LPNs, and NPs reduced cell viability in a concentration-dependent manner (Figure 3). The IC_{50} values of different formulations are shown in Table 2: (1) encapsulation of DTX or CUR to the LPNs exhibited greater cytotoxicity than did free drug formulations ($p < 0.05$); (2) co-encapsulation of DTX and CUR in LPNs significantly reduced cell viability relative to single drug-loaded LPNs ($p < 0.05$), demonstrating the synergistic effect of the combination therapy; (3) cytotoxic effects of DTX-CUR-LPNs were obviously than with DTX-CUR-NPs ($p < 0.05$). This suggests that the lipid shell may enhance the adherence ability of the nanocarriers with the cell membrane due to the similar nature of the lipids and the cell membrane. This characteristic
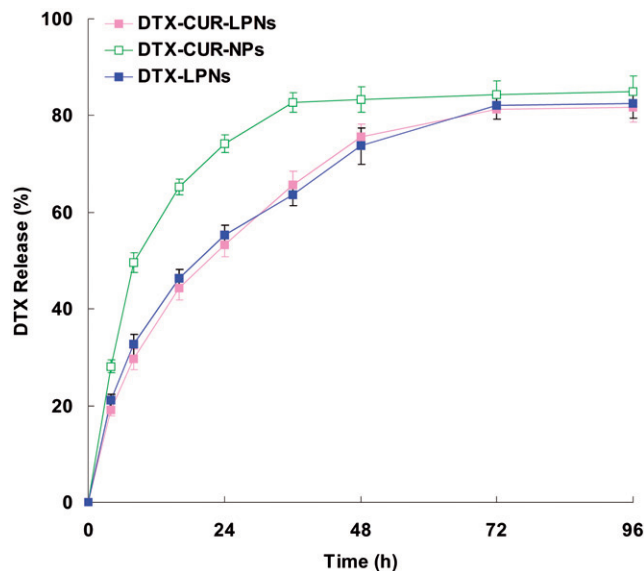

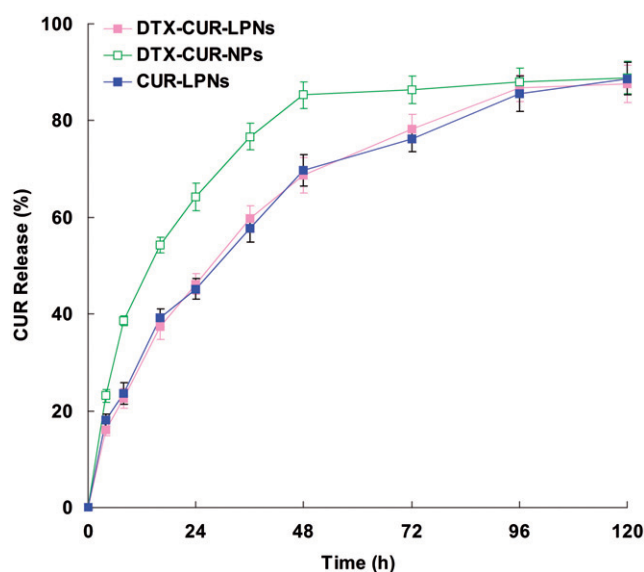Figure 1. *In vitro* release of DTX from different LPNs systems.

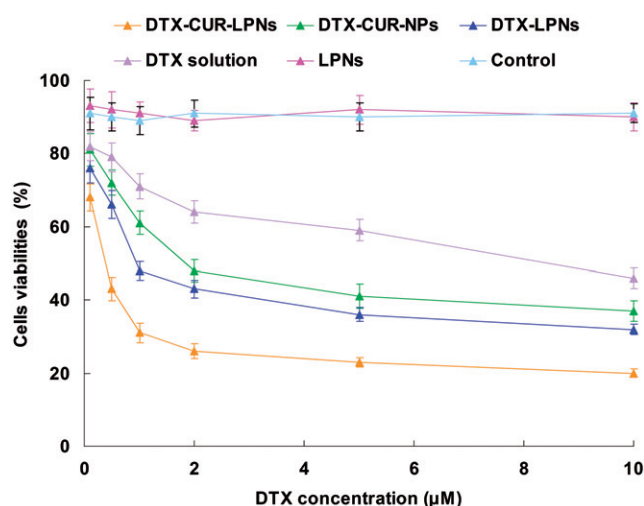Figure 2. *In vitro* release of CUR from different LPNs systems.

Figure 3. *In vitro* cytotoxicity assays of LPNs, NPs, and free drugs.

Table 2. IC$_{50}$ values of different formulations.

Formulations	DTX-CUR-LPNs	DTX-CUR-NPs	DTX-LPNs	CUR-LPNs	Free DTX	Free CUR
IC$_{50}$ DTX (μM)	0.42 ± 0.07	1.81 ± 0.21	0.94 ± 0.16	NA	8.91 ± 0.67	NA
IC$_{50}$ CUR (μM)	0.84 ± 0.12	3.62 ± 0.65	NA	3.62 ± 0.34	NA	16.62 ± 1.13

Table 3. Optimization of DTX to CUR ratios in DTX-CUR-LPNs.

DTX to CUR ratios (w/w)	5:1	2:1	1:1	1:2	1:5
IC$_{50}$ DTX (μM)	1.24 ± 0.36	0.92 ± 0.16	0.89 ± 0.13	0.43 ± 0.08	0.96 ± 0.19
Praticle size (nm)	175.1 ± 5.2	166.5 ± 4.4	168.3 ± 4.2	171.6 ± 3.9	172.4 ± 3.8
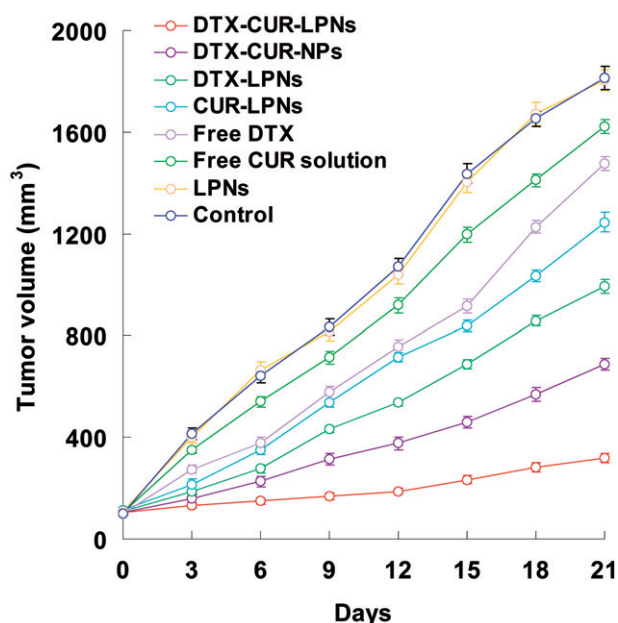
Figure 4. *In vivo* antitumor efficacy of LPNs, NPs, and free drugs.

could enhance the intracellular drug accumulation and exhibit better anticancer efficiency.

Table 3 summarizes the IC$_{50}$ values of DTX-CUR-LPNs when different DTX to CUR ratios were used. The IC$_{50}$ value of the ratio 1:2 were the lowest, this ratio was determined for the preparation of DTX-CUR-LPNs. The size of all the ratios tested appeared to have no significant difference ($p > 0.05$).

In vivo anti-tumor studies of DTX-CUR-LPNs

The *in vivo* antitumor efficacy of LPNs was investigated on the human prostate cancer-bearing Balb/c nude mice model. While tumors grew rapidly in mice injected with the saline control group, all the drug formulations showed efficacy in tumor regression to different extents (Figure 4). Better inhibition of tumor growth was achieved by drug-encapsulated LPNs as compared with the corresponding free drugs ($p < 0.05$); co-delivery of DTX and CUR showed more efficient suppression on tumor growth than the single drug encapsulated LPNs ($p < 0.05$); in comparison with DTX-CUR-NPs, the DTX-CUR-LPNs exhibited the most potent anticancer ability. At the end of the study, the TIR of different groups were calculated. The DTX-CUR-LPNs group

exhibited the highest TIR (82.5%), followed by DTX-CUR-NPs (62.1%) and DTX-LPNs (45.2%). These results could be explained as follows: (1) the structure of LPNs delayed the drug release more than other vectors *in vivo*, and increased the drug accumulation in tumor tissues; (2) the lipid shell of LPNs has high affinity to the lipid structured cell surface, promote the fusion of the nanocarriers to the cell membrane, and deliver more drug into the tumor cells.

Conclusion

In this study, we have described the preparation and characterization of LPNs for co-encapsulation of DTX and CUR. In PC-3 human prostate carcinoma cells, DTX-CUR-LPNs showed greater cytotoxicity than single drug-encapsulated LPNs and free drug solutions. The same results have also been found *in vivo*, on human prostate cancer-bearing Balb/c nude mice. This suggests that co-encapsulation of DTX and CUR using LPNs would be promising for prostate cancer treatment.

Declaration of interest

References

Berthold DR, Pond GR, Soban F, et al. (2008). Docetaxel plus prednisone or mitoxantrone plus prednisone for advanced prostate cancer: updated survival in the TAX 327 study. J Clin Oncol 26: 242–5.

Bissett D, Setanoians A, Cassidy J, et al. (1993). Phase I and pharmacokinetic study of taxotere (RP56976) administered as a 24-hour infusion. Cancer Res 53:523–7.

Burgos-Morón E, Calderón-Montaño JM, Salvador J, et al. (2010). The dark side of curcumin. Int J Cancer 126:1771–5.

Chan JM, Zhang L, Yuet KP, et al. (2009). PLGA-lecithin-PEG core-shell nanoparticles for controlled drug delivery. Biomaterials 30: 1627–34.

Chandratre SS, Dash AK. (2015). Multifunctional nanoparticles for prostate cancer therapy. AAPS PharmSciTech 16:98–107.

Chen QH. (2015). Curcumin-based anti-prostate cancer agents. Anticancer Agents Med Chem 15:138–56.

Dorai T, Diouri J, O'Shea O, et al. (2014). Curcumin inhibits prostate cancer bone metastasis by up-regulating bone morphogenic protein-7 *in vivo*. J Cancer Ther 5:369–86.

Eggen S, Fagerland SM, Mørch Ý, et al. (2014). Ultrasound-enhanced drug delivery in prostate cancer xenografts by nanoparticles stabilizing microbubbles. J Control Release 187:39–49.

Eom DW, Lee JH, Kim YJ, et al. (2014). Synergistic effect of curcumin on epigallocatechin gallate-induced anticancer action in PC3 prostate cancer cells. BMB Rep. [Epub ahead of print]. pii: 2990.

Galsky MD, Vogelzang NJ. (2010). Docetaxel-based combination therapy for castration-resistant prostate cancer. Ann Oncol 21: 2135–44.

Guo H, Xu Y, Fu Q. (2015). Curcumin inhibits growth of prostate carcinoma via miR-208-mediated CDKN1A activation. Tumour Biol. [Epub ahead of print]. doi: 10.1007/s13277-015-3592-y.

Hadinoto K, Sundaresan A, Cheow WS. (2013). Lipid-polymer hybrid nanoparticles as a new generation therapeutic delivery platform: a review. Eur J Pharm Biopharm 85:427–43.

Hajikarimi Z, Khoei S, Khoee S, et al. (2014). Evaluation of the cytotoxic effects of PLGA coated iron oxide nanoparticles as a carrier of 5-fluorouracil and mega-voltage X-ray radiation in DU145 prostate cancer cell line. IEEE Trans Nanobiosci 13:403–8.

Healy SJ, Gorman AM, Mousavi-Shafaei P, et al. (2009). Targeting the endoplasmic reticulum-stress response as an anticancer strategy. Eur J Pharmacol 625:234–46.

Hoang B, Ernsting MJ, Murakami M, et al. (2014). Docetaxel-carboxymethylcellulose nanoparticles display enhanced anti-tumor activity in murine models of castration-resistant prostate cancer. Int J Pharm 471:224–33.

Horie S. (2012). Chemoprevention of prostate cancer: soy isoflavones and curcumin. Korean J Urol 53:665–72.

Jemal A, Bray F, Center MM, et al. (2011). Global cancer statistics. CA Cancer J Clin 61:69–90.

Jin J, Sui B, Gou J, et al. (2014). PSMA ligand conjugated PCL-PEG polymeric micelles targeted to prostate cancer cells. PLoS One 9: e112200.

Li J, Djenaba JA, Soman A, et al. (2012). Recent trends in prostate cancer incidence by age, cancer stage, and grade, the United States, 2001–2007. Prostate Cancer 2012:6913.

Lin SS, Huang HP, Yang JS, et al. (2008). DNA damage and endoplasmic reticulum stress mediated curcumin-induced cell cycle arrest and apoptosis in human lung carcinoma A-549 cells through the activation caspases cascade-and mitochondrial-dependent pathway. Cancer Lett 272:77–90.

Liu C, Zhu Y, Lou W, et al. (2013). Functional p53 determines docetaxel sensitivity in prostate cancer cells. Prostate 73:418–27.

Liu Q, Li J, Pu G, et al. (2015). Co-delivery of baicalein and doxorubicin by hyaluronic acid decorated nanostructured lipid carriers for breast cancer therapy. Drug Deliv. [Epub ahead of print]. doi: 10.3109/10717544.2015.1031295.

Luo Y, Ling Y, Guo W, et al. (2010). Docetaxel loaded oleic acid-coated hydroxyapatite nanoparticles enhance the docetaxel-induced apoptosis through activation of caspase-2 in androgen independent prostate cancer cells. J Control Release 147:278–88.

Mathur A, Abd Elmageed ZY, Liu X, et al. (2014). Subverting ER-stress towards apoptosis by nelfinavir and curcumin coexposure augments docetaxel efficacy in castration resistant prostate cancer cells. PLoS One 9:e103109.

Mehta RS, Barlow WE, Albain KS, et al. (2012). Combination anastrozole and fulvestrant in metastatic breast cancer. N Engl J Med 367:435–44.

Saengkrit N, Saesoo S, Srinuanchai W, et al. (2014). Influence of curcumin-loaded cationic liposome on anticancer activity for cervical cancer therapy. Colloids Surf B Biointerfaces 114:349–56.

Schonthal AH. (2012). Targeting endoplasmic reticulum stress for cancer therapy. Front Biosci (Schol Ed) 4:412–31.

Sundram V, Chauhan SC, Ebeling M, et al. (2012). Curcumin attenuates β-catenin signaling in prostate cancer cells through activation of protein kinase D1. PLoS One 7:e35368.

Vaishampayan U, Hussain M. (2008). Update in systemic therapy of prostate cancer: improvement in quality and duration of life. Expert Rev Anticancer Ther 8:269–81.

van Oosterom AT, Schrijvers D, Schrijvers D. (1995). Docetaxel (Taxotere), a review of preclinical and clinical experience. Part II: clinical experience. Anticancer Drugs 6:356–68.

Wei X, Zhou D, Wang H, et al. (2013). Effects of pyridine analogs of curcumin on growth, apoptosis and NF-κB activity in prostate cancer PC-3 cells. Anticancer Res 33:1343–50.

Woo JH, Kim YH, Choi YJ, et al. (2003). Molecular mechanisms of curcumin-induced cytotoxicity: induction of apoptosis through generation of reactive oxygen species, down-regulation of Bcl-XL and IAP, the release of cytochrome c and inhibition of Akt. Carcinogenesis 24: 1199–208.

Wu Y, Fabritius M, Ip C. (2009). Chemotherapeutic sensitization by endoplasmic reticulum stress: increasing the efficacy of taxane against prostate cancer. Cancer Biol Ther 8:146–52.

Yallapu MM, Khan S, Maher DM, et al. (2014). Anti-cancer activity of curcumin loaded nanoparticles in prostate cancer. Biomaterials 35: 8635–48.

Yang Q, Yang Y, Li L, et al. (2015). Polymeric nanomedicine for tumor-targeted combination therapy to elicit synergistic genotoxicity against prostate cancer. ACS Appl Mater Interfaces 7:6661–73.

Zhang L, Chan JM, Gu FX, et al. (2008). Self-assembled lipid–polymer hybrid nanoparticles: a robust drug delivery platform. ACS Nano 2: 1696–702.

Zhu Y, Liu C, Armstrong C, et al. (2015). Anti-androgens inhibit ABCB1 efflux and ATPase activity and reverse docetaxel resistance in advanced prostate cancer. Clin Cancer Res 2015. [Epub ahead of print]. doi: 10.1158/1078-0432.CCR-15-0269.

Zu S, Ma W, Xiao P, et al. (2015). Evaluation of docetaxel-sensitive and docetaxel-resistant proteomes in PC-3 cells. Urol Int 2015. [Epub ahead of print]. doi: 10.1159/000351263.